Collective Representation of Lower Lying States in Ne^{21}, Na^{21}, and Na^{23}†

A. J. HOWARD,* J. P. ALLEN, AND D. A. BROMLEY
Nuclear Structure Laboratory, Yale University, New Haven, Connecticut
(Received 30 March 1965)

Employing model parameters deduced from the observed static properties of the nuclear systems Ne^{21}, Na^{21}, and Na^{23}, both total and partial gamma-ray transition probabilities involving relevant states in the ground-state rotational bands are computed within the Nilsson strong-coupling collective-model framework and compared with the respective observed values; agreement within a factor of 2 is noted for all cases with the exception of the first-excited to ground-state Ne^{21} transition. Similar comparisons of relative total gamma-ray transition probabilities involving postulated $\frac{9}{2}^+$ members of these same rotational bands are also presented. The relative phases of coherently interfering magnetic-dipole and electric-quadrupole radiation amplitudes are predicted for the pertinent intraband transitions; agreement with the observed relative phases is found in three of the four cases available for unambiguous comparison. Model-predicted values for beta-ray transition probabilities involving the ground states of these three nuclei are in good agreement with observations. These comparisons provide striking support for the model validity for the description of these nuclei; prolate deformations corresponding to $\eta \sim +4.0$ are indicated by these comparisons and in addition by examination of the total nuclear binding energy calculated as a function of deformation.

I. INTRODUCTION

ALTHOUGH numerous attempts to describe odd-A nuclear systems in which the odd nucleon count, hereafter denoted by ζ, is 11, have been carried out previously within strong-coupling collective-model frameworks, the comparison of such interpretations with experimental observations has been almost exclusively limited to static properties primarily because of a paucity of detailed information on the pertinent dynamic-level characteristics.[1-9] Even a meaningful evaluation of these previous interpretations has been partially precluded by the ambiguous nature concerning the majority of the experimental spin-parity assignments for the low-lying excited states in such "central" $\zeta=11$ nuclei as Ne^{21}, Na^{21}, and Na^{23}.

The results of several recent investigations have provided sufficient information concerning the lower lying levels of these three nuclei upon which to base a detailed comparison of the dynamic predictions of a strong-coupling collective model. The Nilsson model[10,11] has been widely applied in describing nuclei located in the $2s$-$1d$ nuclear shell; notable success regarding the interpretation of static nuclear properties has been attained, but presently there are only a few isolated cases where sufficient data have been available to permit examination of the detailed model predictions concerning dynamic properties.[12,13] This paper presents a comparison of the specific Nilsson-model predictions with the currently available data on Ne^{21}, Na^{21}, and Na^{23}.

In a strong-coupling collective-model interpretation of nuclear structure, configuration mixing is primarily attributed to the Coriolis coupling existing between states of the same spin and parity which are members of rotational bands with $|\Delta K| \leq 1$. The strength of this Coriolis coupling is inversely related to the energy separation between pertinent unperturbed members of $|\Delta K| \leq 1$ rotational bands. The energy spacing of unperturbed members of each rotational band is in general sensitively dependent on the moment-of-inertia parameter $\hbar^2/2I$; the excitation energy of each band relative to the "ground state" rotational band is approximately linearly related to the spin-orbit coupling parameter κ within the range thereof pertinent to the $\zeta=11$ nuclei to be investigated herein.

As will be fully discussed in Sec. III of this paper, the four lowest lying positive parity rotational bands predicted for $\zeta=11$ nuclei by the Nilsson model are $K=\frac{3}{2}$, $\frac{1}{2}$, $\frac{1}{2}$, and $\frac{5}{2}$, respectively; Fig. 1 reproduces the relevant section of the Nilsson energy eigenvalue diagram. Hence there are at least four sources of Coriolis coupling to be considered in determining the appropriate model wave

† Work supported in part by the U. S. Atomic Energy Commission.
* Summer Research Associate. Permanent address: Trinity College, Hartford, Connecticut.
[1] E. B. Paul and J. H. Montague, Nucl. Phys. 8, 61 (1958).
[2] J. M. Freeman in *Proceedings of the International Conference on Nuclear Structure, 1960*, edited by D. A. Bromley and E. Vogt (University of Toronto Press, Toronto, 1960), p. 447.
[3] T. H. Kruse, R. D. Bent, and L. J. Lidofsky, Phys. Rev. 119, 289 (1960).
[4] A. B. Clegg and K. J. Foley, Phil. Mag. 7, 247 (1962).
[5] R. D. Bent, J. E. Evans, G. C. Morrison, and I. J. Van Heerden in *Proceedings of the Third Conference on Reactions Between Complex Nuclei*, edited by A. Ghiorso, R. M. Diamond, and H. E. Conzett (University of California Press, Berkeley and Los Angeles, 1963), p. 417.
[6] B. E. Chi and J. P. Davidson, Phys. Rev. 131, 366 (1963); B. E. Chi, Doctoral dissertation, Rensselaer Polytechnic Institute, 1963 (unpublished); J. R. Roesser, Doctoral dissertation, Rensselaer Polytechnic Institute, 1964 (unpublished).
[7] R. M. Dreizler, Phys. Rev. 132, 1166 (1963).
[8] W. Glöckle, Z. Physik 178, 53 (1964).
[9] I. Kelson and C. A. Levinson, Phys. Rev. 134, B269 (1964); C. A. Levinson, *ibid.* 132, 2184 (1963); I. Kelson, *ibid.* 132, 2189 (1963).
[10] S. G. Nilsson, Kgl. Danske Videnskab. Selskab, Mat. Fys. Medd. 29, No. 16 (1955).
[11] B. R. Mottelson and S. G. Nilsson, Kgl. Danske Videnskab. Selskab, Mat. Fys. Skrifter 1, No. 8 (1959).
[12] A. E. Litherland, H. McManus, E. B. Paul, D. A. Bromley, and H. E. Gove, Can. J. Phys. 36, 378 (1958).
[13] G. J. McCallum, Phys. Rev. 123, 568 (1961).

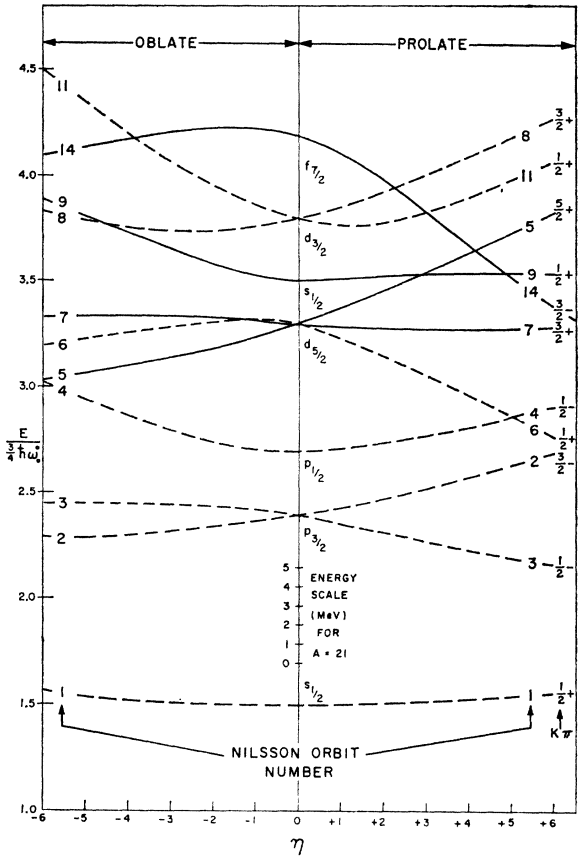

FIG. 1. Energy levels of the Nilsson model (Refs. 10 and 11) as functions of the deformation parameter η for $\kappa=0.10$. The integers adjacent to the levels indicate the associated Nilsson orbit number. The levels are identified at zero deformation via spherical-shell-model notation and at nonzero deformation by the values of Ω and π for the orbit. The orbitals for the extra-core nucleon discussed in the text are indicated by the solid curves.

functions for the lower lying states in these nuclear systems.

Of the previously mentioned calculations which investigated the effects of Coriolis coupling as regards the low-lying energy spectrum for one or more of the three $\zeta=11$ nuclei to be treated herein, the recent presentations of Glöcke[8] and of Kelson and Levinson[9] are the most detailed in this respect. Both of these calculations (as well as the other calculations cited earlier) indicate that the three lowest lying states in each of Ne^{21}, Na^{21}, and Na^{23} are predominantly $K^\pi=\frac{3}{2}^+$ configurations corresponding to location of the extra-core nucleon in Nilsson orbit 7 above respective Ne^{20}, Ne^{20}, Ne^{22} core configurations: Empirical evidence on the aforementioned states is summarized in Fig. 2 and Table I. Glöcke[8] considered the interactions among the three lowest lying "single-particle" bands and the lowest lying "hole" band predicted by the Nilsson model for $\zeta=11$ nuclear systems; the energy separations of these four bands are estimated in Fig. 3. The values for moment-of-inertia and spin-orbit coupling parameters employed by Glöcke were the same for each of the four bands considered in his treatment of the Na^{23} energy spectrum: $\hbar^2/2I=0.25$ MeV and $\kappa=0.07$. Kelson and Levinson[9] included only the three "single-particle" bands mentioned above in their determinations; common parametric values $\hbar^2/2I=0.19$ MeV and $\kappa\simeq0.12$ were used to describe all three bands in their treatment of Na^{23}.

Typical of all the previous presentations cited above, the two calculations just discussed generate model wave functions for the lowest lying $\frac{3}{2}^+$, $\frac{5}{2}^+$, and $\frac{7}{2}^+$ states which are characterized by predominant $K=\frac{3}{2}$ amplitudes of approximately $+0.98$, $+0.85$, and $+0.80$, respectively, in each of the systems under discussion. However, the values for each of the smaller "contaminant" amplitudes deduced in these two calculations are decidedly different, reflecting not only the neglect of the "hole" band in one of these two analyses but also the employment of different values of the moment-of-inertia and spin-orbit coupling parameters in these two calculations.

Difficulties in an accurate estimate of the moment of inertia for the mass-21 and mass-23 configurations treated herein via relationship to the respective values deduced for the Ne^{20} and Ne^{22} "core" configurations have been thoroughly discussed by Kelson and Levinson.[9] These difficulties are compounded by the uncertainties associated with the related "core" parameters themselves: Present evidence delimits $\hbar^2/2I$ to $+0.24\pm0.02$ MeV for Ne^{20} and $+0.19\pm0.03$ MeV for Ne^{22} (note also that $\hbar^2/2I=+0.21\pm0.02$ for Mg^{24}). The present uncertainty associated with the appropriate value for the spin-orbit coupling parameter κ in the Nilsson-model description of $\zeta=11$ nuclear systems will

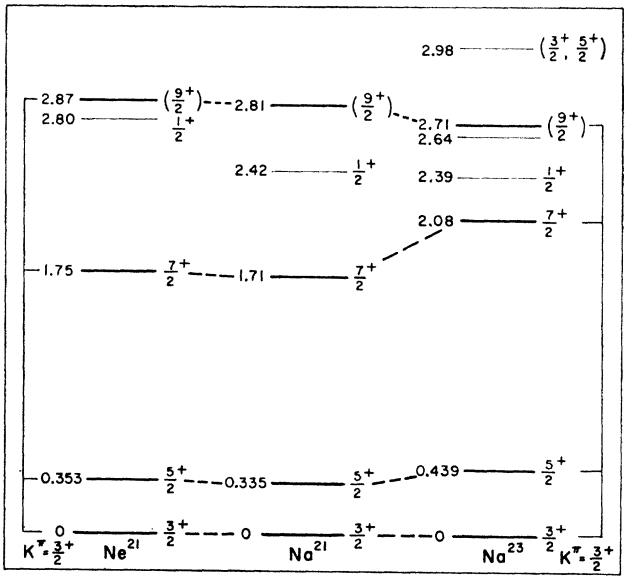

FIG. 2. Energy-level diagrams for Ne^{21}, Na^{21}, and Na^{23} up to 3-MeV excitation. States interpreted as members of the $K^\pi=\frac{3}{2}^+$ rotational band based on Nilsson orbit 7 are indicated (see also Table I).

be discussed in Sec. III of this paper. Variation of these two model parameters (i.e., $\hbar^2/2I$ and κ) upon which the degree of Coriolis coupling is most strongly dependent within the ranges defined by their present uncertainties for the configurations mentioned above drastically affects the amplitudes for each of the several "contaminants" in the model-predicted wave functions for each of the lower lying states in Ne^{21}, Na^{21}, and Na^{23} which are predominantly members of the lowest lying $K^\pi=\frac{3}{2}^+$ rotational band. The sensitivity of the Coriolis coupling strengths to these two model parameters in $\zeta=11$ nuclear systems is most concisely illustrated by the proximate excitation energy for each of the pertinent "contaminant" rotational bands as demonstrated in Fig. 3.

It is concluded from a detailed scrutiny of the aforementioned calculations that (1) *upper* limits of 4%, 27%, and 35% can be reasonably applied to the *total* contaminant intensities associated with the respective wave function for the three lowest lying $\frac{3}{2}^+$, $\frac{5}{2}^+$, and $\frac{7}{2}^+$ states in each of Ne^{21}, Na^{21}, and Na^{23} (see Fig. 2) and (2) meaningful subdivision of the total contaminant amplitude into fractions associated with each of the three pertinent bands for the aforementioned $\frac{5}{2}$ and $\frac{7}{2}$ state wave functions cannot be presently carried out because of uncertainties in both the values associated with the relevant model parameters discussed above and the J^π characteristics for the higher lying states in these three systems.

In view of these conclusions, the most tenable interpretation of the dynamic properties of the lower lying states in Ne^{21}, Na^{21}, and Na^{23} presently obtainable involves neglect of the several "contaminant" amplitudes in the wave functions for these states; the best justification for this approximation is the *a posteriori* one obtained by treating the lowest lying $J^\pi=\frac{3}{2}^+$, $\frac{5}{2}^+$, and $\frac{7}{2}^+$ states in each of Ne^{21}, Na^{21}, and Na^{23} as uncontaminated members of the $K^\pi=\frac{3}{2}^+$ rotational band based upon location of the extra-core nucleon in Nilsson orbit 7.

As regards the $J^\pi=\frac{3}{2}^+$ ground state in each of Ne^{21}, Na^{21}, and Na^{23}, all of the aforementioned interpretations indicate $K^\pi=\frac{3}{2}^+$ (Nilsson orbit 7) wave-function amplitude purity $\gtrsim 0.98$ ($\gtrsim 96\%$ intensity). Therefore, the inclusion of only the $K^\pi=\frac{3}{2}^+$ amplitude of the ground-state wave function in the treatment of such observed static properties as the electric-quadrupole and magnetic-dipole moments appears quite reasonable. Model parameters deduced from such treatments must, within the model definition, be applicable to the higher lying members of this rotational level in the present consideration.

TABLE I. Observed states interpreted as members of $K^\pi=\frac{3}{2}^+$ rotational band based on Nilsson orbit 7.

Band member k	J_k	Excitation energy, E_k (MeV) Ne^{21}	Na^{21}	Na^{23}
1	$\frac{3}{2}$	0	0	0
2	$\frac{5}{2}$	0.353	0.335	0.439
3	$\frac{7}{2}$	1.75	1.71	2.08
4	$\frac{9}{2}$	(2.87)[a]	(2.81)[a]	(2.71)[a]

[a] Tentative assignment.

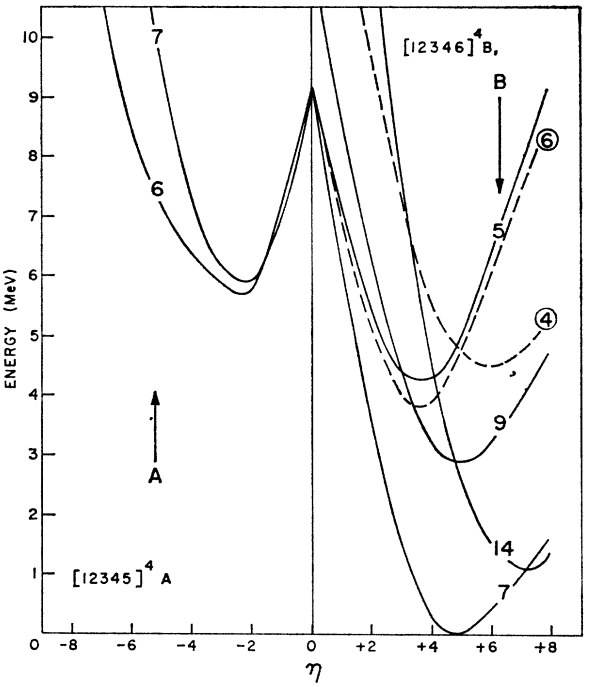

FIG. 3. Total (normalized) nuclear binding energy versus the core-deformation parameter η for pertinent low-lying single-particle configurations of Ne^{21} and Na^{21} (solid curves). The minimum energy is associated with the $[12346]^4\,7$ configuration for $\eta\simeq+4.8$, and energies are presented as excitations above this minimum energy. The dashed curves represent the excitation energies associated with the lowest lying positive- and negative-parity hole configurations, which are formed by promotion of a core nucleon from Nilsson orbits 6 and 4, respectively, into Nilsson orbit 7.

In summary, the dynamic properties associated with the lowest lying $\frac{3}{2}^+$, $\frac{5}{2}^+$, and $\frac{7}{2}^+$ states in each of Ne^{21}, Na^{21}, and Na^{23} are deduced within the Nilsson-model framework by first obtaining relevant parameter values from considerations of the observed static properties of the ground states in each system and then treating the aforementioned states as $K^\pi=\frac{3}{2}^+$ rotational band members, neglecting "contamination" amplitudes in the wave functions caused by Coriolis coupling.

II. SUMMARY OF PERTINENT SPECTROSCOPIC DATA

The experimental observations upon which the ensuing intercomparison is based are summarized herein: The static properties of the relevant states in Ne^{21}, Na^{21}, and Na^{23} are presented in Fig. 2, Table I, and Table II. The spin-parity assignments and dynamic properties of the excited states of interest in Ne^{21}, Na^{21}, and Na^{23} are discussed in this section, and pertinent beta-ray transition probability data are presented in Sec. III in tabular form together with the model predictions.

TABLE II. Ground-state electric-quadrupole and magnetic-dipole moments.

Nucleus	Q_s (barns) Observed	Ref.	Predicted[a] $\kappa=0.05$	$\kappa=0.10$	μ (nuclear magnetons) Observed	Ref.	Predicted[a] $g_R=0.23$	$g_R=0.48$
Ne^{21}	$+0.093\pm0.010$	30	$+0.039$	$+0.089$	-0.662	33	-0.858	-0.708
Na^{23}	$+0.101\pm0.011$	31	$+0.044$	$+0.106$	$+2.216$	34	$+2.232$	$+2.382$

[a] Computed with $\eta=+4.0$.

A. Ne^{21}

Unambiguous J^π assignments for the four lowest lying states in Ne^{21}, namely the ground, 0.353-, 1.75-, and 2.80-MeV states, have recently been established as $\frac{3}{2}^+$, $\frac{5}{2}^+$, $\frac{7}{2}^+$, and $\frac{1}{2}^+$, respectively, on the basis of several reported observations; a detailed summary of these measurements is available elsewhere.[14] There also exists weak evidence from the observed branching ratio of the 2.87-MeV Ne^{21} state that this may represent a $\frac{9}{2}^+$ configuration.[14,15] In terms of the phase convention introduced by Lloyd and defined in Sec. IIIE, the multipole amplitude ratio for the $\frac{5}{2}^+$(0.353-MeV) $\rightarrow\frac{3}{2}^+$ (ground-state) Ne^{21} transition has been determined by Deuchars and Dandy,[16] via studies on the $O^{18}(\alpha,n\gamma)Ne^{21}$ reaction, to be $+0.004\leq\delta_{21}\leq+0.03$; this same quantity has been delimited from previously reported studies on the $Ne^{20}(d,p\gamma\gamma)Ne^{21}$ reaction[14] as $-0.02\leq\delta_{21}\leq+0.03$. The multipole amplitude ratio for the $\frac{7}{2}^+$(1.75-MeV)$\rightarrow$ $\frac{5}{2}^+$(0.353-MeV)Ne^{21} de-excitation radiation[17] has been measured as $+0.12\leq\delta_{32}\leq+0.18$ from studies on the $F^{19}(He^3,p\gamma)Ne^{21}$ reaction by Pelte *et al.*,[15] but $-0.17\leq\delta_{32}\leq-0.11$ from the aforementioned $Ne^{20}(d,p\gamma\gamma)Ne^{21}$ studies.[14] Branching ratio determinations indicate that the 1.75-MeV Ne^{21} state de-excites with $94\pm1\%$ and $93\pm1\%$ relative intensity via the $\frac{7}{2}^+\rightarrow\frac{5}{2}^+$ cascade transition in these two latter studies. The $(\frac{9}{2}^+)$(2.87-MeV) state has been observed to de-excite $\sim50\%$ and $>50\%$ to the $\frac{7}{2}^+$(1.75-MeV)Ne^{21} state in these respective investigations. The total lifetime of the first-excited state in Ne^{21} was measured to be $(6.2\pm6.2)\times10^{-11}$ sec from studies on the $O^{18}(\alpha,n\gamma\gamma)Ne^{21}$ reaction by Khabakhpashev and Tsenter,[18] and an observed $E2$ partial lifetime of 9.2×10^{-10} sec is reported from Coulomb excitation studies carried out by Andreev *et al.*[19] The total lifetimes of the 1.75-, 2.80-, and 2.87-MeV Ne^{21} states have recently been reported by Bent *et al.*[5] as $0.20_{-0.13}{}^{+0.23}$, $0.23_{-0.13}{}^{+0.20}$, ~0.1 psec, respectively, from investigation of the $O^{16}(Be^9,\alpha\gamma)Ne^{21}$ reaction.

B. Na^{21}

In the case of Na^{21}, mirror-pair arguments in conjunction with numerous experimental observations, as summarized by Ajzenberg *et al.*,[20] indicate $J^\pi=\frac{3}{2}^+$, $\frac{5}{2}^+$, $\frac{7}{2}^+$, and $\frac{1}{2}^+$ assignments to the ground, 0.353-, 1.71-, and 2.42-MeV Na^{21} states; these results are corroborated by analysis of the results of $Ne^{20}(p,\gamma)Na^{21}$ and $Ne^{20}(d,p')$-Ne^{21} studies recently carried out.[21,22] The multipole amplitude ratio for the $\frac{5}{2}^+$(0.335-MeV) $\rightarrow\frac{3}{2}^+$ (ground-state) transition has been determined by van der Leun and Mouton[23] via studies on the $Ne^{20}(p,\gamma)Na^{21}$ reaction to be $0\leq\delta_{21}\leq+0.10$; the multipole amplitude ratio has not as yet been reported for the $\frac{7}{2}^+$(1.71-MeV) $\rightarrow$ $\frac{5}{2}^+$(0.335-MeV)Na^{21} transition. Other studies on the $Ne^{20}(p,\gamma)Na^{21}$ reaction have determined the branching ratio for the de-excitation radiations from the $\frac{7}{2}^+$(1.71-MeV)Na^{21} state to be $89\pm2\%$ relative intensity to the $\frac{5}{2}^+$(0.335-MeV)Na^{21} state.[21,22] Consistent with the current (limited) data thereon, the 2.84-MeV Na^{21} state is identified as the mirror-pair analog of the $(\frac{9}{2}^+)$(2.87-MeV)Ne^{21} state. No lifetime measurements on these Na^{21} states have been reported.

C. Na^{23}

Unambiguous J^π assignments of $\frac{3}{2}^+$, $\frac{5}{2}^+$, and $\frac{7}{2}^+$ have been reported by Braben *et al.*[24] for the respective ground-, 0.439-, and 2.08-MeV Na^{23} states. The total mean lifetime for the first-excited state in Na^{23} has been determined by Rasmussen *et al.*[25] to be $(1.8_{-0.3}{}^{+0.4})\times10^{-12}$ sec, and the partial mean lifetime against electric quadrupole de-excitation has been reported by Temmer

[14] A. J. Howard, D. A. Bromley, and E. K. Warburton, Phys. Rev. **137**, B32 (1965).
[15] D. Pelte, B. Povh, and W. Scholz, Nucl. Phys. **55**, 322 (1964).
[16] W. M. Deuchars and D. Dandy, Proc. Phys. Soc. (London) **77**, 1197 (1961).
[17] The previously reported (Refs. 14, 15) agreement in the determinations of the multipole amplitude ratio for the 1.75- $\rightarrow$ 0.353-MeV Ne^{21} transition by Howard *et al.* (Ref. 14) and Pelte *et al.* (Ref. 15) is incorrect; while the magnitudes determined are nearly the same, the relative phases measured are opposite. See Sec. IIIE.
[18] A. G. Khabakhpashev and E. M. Tsenter, Izv. Akad. Nauk SSSR Ser. Fiz. **23**, 883 (1959); and Zh. Eksperim. i Teor. Fiz. **37**, 991 (1959) [English transl.: Soviet Phys.—JETP **10**, 705 (1960)].
[19] D. S. Andreev, E. I. Erokhina, and I. Kh. Lemberg, Izv. Akad. Nauk SSSR Ser. Fiz. **23**, 1470 (1959).
[20] F. Ajzenberg-Selove, L. Cranberg, and F. S. Dietrich, Phys. Rev. **124**, 1548 (1961).
[21] A. J. Howard, J. P. Allen, D. A. Bromley, and E. K. Warburton (to be published).
[22] J. P. Allen, Doctoral dissertation, Yale University, 1965 (unpublished).
[23] C. van der Leun and W. L. Mouton, Physica **30**, 333 (1964).
[24] D. W. Braben, L. L. Green, and J. C. Willmott, Nucl. Phys. **32**, 584 (1962).
[25] V. K. Rasmussen, F. R. Metzger, and C. P. Swann, Nucl. Phys. **13**, 95 (1959).

and Heydenburg[26] to be 4.3×10^{-10} sec.[27] Assuming a 10% uncertainty in this latter value, the absolute value of the multipole amplitude ratio for the $\frac{5}{2}^+$(0.439-MeV) $\rightarrow \frac{3}{2}^+$ (ground-state) transition computed from these lifetime measurements is restricted to the range $0.056\leq|\delta_{21}|\leq0.075$. The angular distribution and direction-polarization measurements on the 0.439-MeV gamma radiation from the $Na^{23}(p,p'\gamma)Na^{23}$ reaction by Mizobuchi *et al.*[28] have indicated this multipole amplitude ratio to be $+0.03\leq\delta_{21}\leq+0.06$, which agrees in magnitude with the value computed directly from the measured lifetimes within the experimental uncertainties and which additionally determines the relative phase of the dipole and quadrupole components in the transition. Since several other independent determinations of δ_{21} are within the range specified by the delimitation established by Mizobuchi *et al.*,[28] the empirical value $\delta_{21}=+0.045\pm0.015$ will be assumed herein.[29]

Employing the aforementioned value for δ_{21}, the multipole amplitude parameter for the $\frac{7}{2}^+$(2.08-MeV) $\rightarrow$ $\frac{5}{2}^+$(0.439-MeV)Na^{23} transition has recently been restricted to the regions $+0.22\leq\delta_{32}\leq+0.60$ or $+1.3\leq\delta_{32}\leq+2.5$ by gamma-gamma angular correlation studies following population of the 2.08-MeV Na^{23} state via the $Ne^{23}(\beta^-)Na^{23*}$ reaction.[29] These investigations also established a branching ratio of $97\pm3\%$ relative intensity for the $\frac{7}{2}^+$(2.08-MeV) $\rightarrow$ $\frac{5}{2}^+$(0.439-MeV)Na^{23} transition.

Based on evidence similar to that for the 2.87-MeV Ne^{21} state, the 2.71-MeV Na^{23} state has been tentatively assigned $J^\pi=(\frac{9}{2}^+)$: It has been reported by Kruse *et al.*[3] from $Na^{23}(p,p'\gamma)Na^{23}$ studies that the 2.71-MeV Na^{23} state de-excites to both the $\frac{7}{2}^+$(2.08)-MeV and $\frac{5}{2}^+$(0.439)-MeV Na^{23} states, with 72% relative intensity for the former transition.

III. NILSSON-MODEL INTERPRETATION

In generating predictions for gamma-ray transition probabilities within the Nilsson-model framework,[10] it is necessary to select values for the nuclear deformation, spin-orbit coupling, and core-gyromagnetic-ratio parameters which are in reasonable agreement with the corresponding values deduced from considerations of static nuclear properties. The nuclear deformation, parametrized herein by η, for low-lying states is commonly estimated from the sign and magnitude of the ground-state electric-quadrupole moment and/or the identified band sequence associated with the observed excited-level spectrum; the strength of the spin-orbit coupling, parametrized by κ, is also usually obtained from the ground-state electric-quadrupole moment, whereas the core-gyromagnetic-ratio g_R can be expressed in an approximate fashion in terms of the ground-state magnetic-dipole moment.[11] In the following subsections, deductions of the values for these three model parameters are carried out from static property considerations, and the resulting values are then used to predict certain dynamic properties associated with low-lying states.

A. The Nuclear Deformation

Calculations[10–12] of the model spectrum in a spheroidal, pure oscillator potential, characteristic of the Nilsson model, establish that for the $\zeta=11$ nuclei the lowest energy state available for the last (unpaired) nucleon is dependent upon the nuclear deformation in the following fashion for the choice of the spin-orbit coupling parameter κ to be discussed below (Sec. IIIB), namely $\kappa=+0.10$: For $-8\lesssim\eta\lesssim-1.5$, it is the $\Omega^\pi=\frac{1}{2}^+$ state corresponding to Nilsson orbit 6; for $-1.5\lesssim\eta\lesssim+6.5$, it is the $\Omega^\pi=\frac{3}{2}^+$ state corresponding to Nilsson orbit 7; for $+6.5\lesssim\eta\lesssim+11$, it is the $\Omega^\pi=\frac{1}{2}^-$ state corresponding to Nilsson orbit 14. This is shown in Fig. 1, which indicates the energy of an *individual* particle in the spheroidal, pure oscillator potential and where

$$E_j/\tfrac{3}{4}\hbar\omega_0{}^0=(N_j+\tfrac{3}{2})[1-\tfrac{1}{3}\epsilon^2-(2/27)\epsilon^3]^{-1/3}+\kappa r_j(\epsilon), \quad (1)$$

E_j being the energy eigenvalue of the total Hamiltonian. κ, η, and ϵ are interrelated by the following expression:

$$\kappa\eta=\epsilon[1-\tfrac{1}{3}\epsilon^2-(2/27)\epsilon^3]^{-1/3}. \quad (2)$$

In Fig. 1, $N=0$, 1, and 2 states are presented (N is the principal quantum number of the orbit), as is the $N=3$ state (orbit 14) of pertinence in discussing the energy spectra below 5-MeV excitation in the nuclei under consideration.

The observation of the $J^\pi=\frac{3}{2}^+$, $\frac{5}{2}^+$, $\frac{7}{2}^+$ sequence for the three lowest lying states in Ne^{21}, Na^{21}, and Na^{23} (cf. Fig. 2) has been interpreted previously as indicating $-1.5\lesssim\eta\lesssim+6.5$ for these nuclei, and considerations of the observed electric-quadrupole moments for the Ne^{21} and Na^{23} ground states further indicate $\eta>+3$ (see subsection B below). Several strong-coupling-model calculations[1–4] applied primarily to the static properties of these three nuclear systems have also assumed orbit assignments to higher lying positive-parity states; such interpretations have generally been most successful for nuclear deformations characterized by $+3\lesssim\eta\lesssim+4$.

An *estimate* of the equilibrium nuclear shape for the Ne^{21}–Na^{21} mirror pair has been carried out by summing the individual model energy eigenvalues illustrated in Fig. 1 for the 21 nucleons therein. The results for the total system binding energy are presented in Fig. 3, wherein the energy ordinate has been arbitrarily normalized to an excitation scale. In agreement with the considerations just discussed, a prolate equilibrium

[26] G. M. Temmer and N. P. Heydenburg, Phys. Rev. **104**, 989 (1956).

[27] Since completing this work, it has come to our attention that there is a more recent determination of this $E2$ lifetime by P. H. Stelson and F. K. McGowan, Nucl. Phys. **16**, 92 (1960): $\tau(E2)=(6.2\pm1.2)\times10^{-10}$ sec. The conclusions reached herein are not significantly altered if this value is employed in the analyses.

[28] A. Mizobuchi, T. Katoh, and J. Ruan, J. Phys. Soc. (Japan) **15**, 1737 (1960).

[29] A. J. Howard, J. P. Allen, D. A. Bromley, and J. W. Olness, Bull. Am. Phys. Soc. **9**, 68 (1964); and (to be published).

deformation is indicated for the ground-state rotational band with the extra-core nucleon located in Nilsson orbit 7 ($\Omega^\pi=\frac{3}{2}^+$); the core in this case is composed of 20 nucleons, four each in Nilsson orbits 1, 2, 3, 4, and 6 and this nuclear configuration is abbreviated $[12346]^4$ 7. The equilibrium deformation is characterized by $\eta\simeq+4.8$. Considering the approximate nature of this calculation, the agreement with the aforementioned considerations is adequate.

The results of promoting the extra-core nucleon into Nilsson orbits 5, 9, and 14, for which $\Omega^\pi=\frac{5}{2}^+$, $\frac{1}{2}^+$, and $\frac{1}{2}^-$, respectively, yield the higher lying potential-energy curves, still indicating prolate equilibrium deformations, displayed by the appropriately labeled solid curves in Fig. 3. As has been discussed elsewhere,[14] relatively high cross sections for the formation of such states are anticipated to be associated with the (d,p) reaction at and below the relevant Coulomb barrier energy. Since both previous experimental observations and model predictions indicate that the 2.80-MeV Ne^{21} state is the only $J^\pi=\frac{1}{2}^+$ single-particle configuration below approximately 5-MeV excitation energy, recent studies on the $Ne^{20}(d,p\gamma)Ne^{21}$ reaction have suggested that the $\frac{1}{2}^+$(2.80-MeV)Ne^{21} state may be interpreted as being associated with a $[12346]^4$ 9 configuration. It is therefore noteworthy that the present calculation indicates the excitation energy of the corresponding band head as $\sim$2.8 MeV. The severe interband Coriolis mixing discussed in the Introduction, on the other hand, is anticipated to impair the identification of higher spin states from considerations equivalent to those presented above. Available information on the $\frac{5}{2}^+$(3.74-MeV)Ne^{21} state is, however, consistent with the interpretation that it is predominantly the band head of the $[12346]^4$ 5 rotational band; the estimated excitation energy of this band head is $\sim$4.2 MeV.

The relatively high cross section for the formation of the $\frac{3}{2}^-$(4.73-MeV) Ne^{21} state by the (d,p) reaction at and below the Coulomb barrier energy supports the interpretation of this state as being the lowest lying member of a distorted $K^\pi=\frac{1}{2}^-$ rotational band based on Nilsson orbit 14 (i.e., the $[12346]^4$ 14 configuration). As seen in Fig. 3, the estimated equilibrium distortion for this configuration is $\eta\sim+7.4$, significantly larger than the values calculated for the three positive-parity configurations discussed above, and the excitation energy is computed to be $\sim$1.1 MeV, which is also clearly at variance with the observed value. It is important to note that all the computations thus far presented herein were carried out assuming a spheroidal, pure oscillator potential, parametrized by $\mu=0$ in the Nilsson notation, and a spin-orbit interaction characterized by $\kappa=0.10$. As regards the potential form, the choice of $\mu=0$ is consistent with the Nilsson value for states having the principal quantum number $N\leq2$; the spin-orbit interaction strength, parametrized by $\kappa=0.10$, has been selected from considerations of the ground-state properties (see Sec. IIIB). Since $N=3$ for the extra-core nucleon in the $[12346]^4$ 14 configuration, these choices of μ and/or κ may well not be particularly appropriate for the extra-core nucleon in this case. If κ for this nucleon is diminished towards the value 0.05 characteristically associated with $N\geq3$ nucleons, the excitation energy of the associated orbital increases significantly, as can be seen from the three $\mu=0$ excitation-energy curves in Fig. 4. The effect of introducing a square-well contribution to the potential is to depress the excitation energy slightly, as can be seen from the $\kappa=0.05$, $\mu=0$ and 0.35 curves in Fig. 4. In summary, by reducing the spin-orbit interaction parameter for the extra-core, $N=3$ nucleon in Nilsson orbit 14 to a value more consistent with observations on $N=3$ shell nuclei, the observed excitation energy of the lowest lying negative-parity states in $\zeta=11$ nuclei is in satisfactory agreement with the $[12346]^4$ 14 configuration assignment.

In addition to the states formed by promotion of the extra-core nucleon into higher lying orbitals, considerations of hole states is also relevant. The total binding energies of the lowest lying positive- and negative-parity hole states in the mass-21 system, corresponding to $[12346]^4[6]^3[7]^2$ and $[1236]^4[4]^3[7]^2$ configurations, respectively, are indicated by the dashed curves in Fig. 3. Concerning the former configuration, there is as

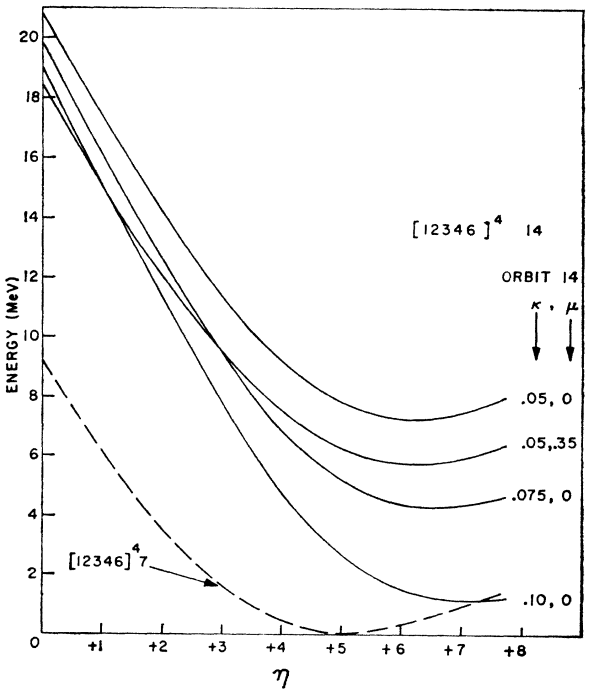

FIG. 4. Excitation energies deduced from total binding energy considerations of the $[12346]^4$ 14 negative-parity configuration for various choices of the spin-orbit coupling strength and the nuclear potential form for the extra-core nucleon. The excitation energies (solid curves) are presented relative to the minimum energy associated with the $[12346]^4$ 7 configuration (dashed curve).

yet no evidence for the existence of a $J^\pi=\frac{1}{2}^+$ (hole) state near 3.8-MeV excitation energy in Ne^{21}; however, several states exist in the vicinity of this excitation energy which are relatively weakly populated in the aforementioned $Ne^{20}(d,p\gamma)Ne^{21}$ studies and for which the J^π characteristics are undetermined at present.[14] As regards the negative-parity hole configuration, the predicted excitation energy closely corresponds to that of the observed $\frac{3}{2}^-$(4.73-MeV)Ne^{21} state. However, the cross-section arguments presented earlier concerning this state are not in accord with this possible hole interpretation.

If pair coupling is assumed to play an important role in the generation of stable nuclear core deformations, the deformation situations in the mass-21 and mass-25 systems should be similar. Since pair coupling is proportional to the number of pairs present in an unfilled shell or subshell, designated as $n/2$, with n representing the lesser value of the number of particles and the number of holes in the unfilled shell or subshell, its importance in the $2s$-$1d$ shell is most pronounced for the nuclei under consideration: The $d_{5/2}$ subshell, capable of containing three pairs each of both protons and neutrons, is characterized by $n_{\max}=3$, whereas $n=2$ for Ne^{21} and Na^{21} as well as for Mg^{25} and Al^{25}. For Na^{23}, $n=3$. Since $\eta\simeq+4$ previously has been shown to be most successful in describing the mass-25 system,[12] further confidence is placed in the limitations on η presented herein for the mass-21, $\zeta=11$ members.

In summary, there exists substantial evidence for a stable nuclear deformation characterized by $+3\lesssim\eta\lesssim+5$ as being appropriate to a Nilsson-model description of the three $\zeta=11$ nuclei under discussion.

B. Spin-Orbit Coupling

The strength of the spin-orbit coupling term in the nuclear potential, directly proportional to κ in the Nilsson notation, is most realistically estimated for rotational band levels based upon the ground state by considering the observed static electric-quadrupole moment for a given system. Since $Q_s=+(0.093\pm0.010)$ and $+(0.101\pm0.011)$ b are the measured values[30,31] for the ground-state electric-quadrupole moments of Ne^{21} and Na^{23}, respectively, the relationship[10,11]

$$Q_s=\frac{3K^2-J(J+1)}{(J+1)(2J+3)}1.15ZA^{2/3}\times\epsilon(1+\tfrac{1}{2}\epsilon+\cdots)\times10^{-26}\ \text{cm}^2 \quad (3)$$

indicates $\kappa\eta\simeq+0.40$ for both cases. For η restricted to the region of values discussed in subsection A above, namely $+3\lesssim\eta\lesssim+5$, the corresponding spin-orbit strength deduced is limited to $+0.13\gtrsim\kappa\gtrsim+0.08$.

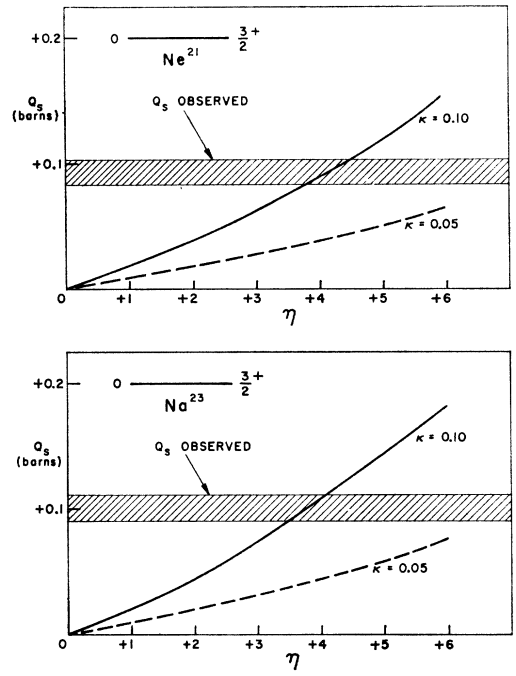

FIG. 5. The electric-quadrupole moments for the ground states of Ne^{21} (upper portion) and Na^{23} (lower portion) versus the core-deformation parameter η. The solid and dashed curves correspond to the Nilsson-model predictions with $\kappa=0.10$ and 0.05, respectively; the cross-hatched regions indicate experimental observations reported in Refs. 30 and 31. See also Table II.

Figure 5 compares the model predictions with experiment. As in the case of η, systematic behavior, as adduced from adjacent odd-A nuclear systems, is consistent with this κ restriction. For the $\zeta=13$ system, $\kappa=+0.08$ has been shown to be most successful in describing the properties of the low-lying levels therein, while for the $\zeta=9$ nucleus O^{17}, there is direct evidence that $\kappa=0.13$ is the most appropriate value.[12] In general, the originally suggested approximation $\kappa=+0.05$ for nuclei beyond the $2s$-$1d$ nuclear shell is recognized to result from Nilsson's attempt[11] to obtain a best fit to the Klinkenberg shell-model level ordering[32] over the entire periodic table with a single averaged κ value; present evidence unambiguously suggests that this average value represents an underestimation for nuclei within this shell. In the absence of any indications to the contrary, it appears reasonable to assume that κ is smoothly varying at the beginning of the $2s$-$1d$ nuclear shell: In consequence of this assumption, a value $\kappa=+0.10$ for the $\zeta=11$ systems is a tenable choice, which, in accordance with the electric-quadrupole moments observed for Ne^{21} and Na^{23}, corresponds to a nuclear deformation of $\eta\cong+4.0$ (cf. Fig. 5 and Table II). These values of κ and η have therefore been selected for the ensuing calculations.

[30] G. M. Grosof, P. Buck, W. Lichten, and I. I. Rabi, Phys. Rev. Letters **1**, 214 (1958).
[31] M. L. Perl, I. I. Rabi, and B. Senitzky, Phys. Rev. **98**, 611 (1955).
[32] P. F. A. Klinkenberg, Rev. Mod. Phys. **24**, 63 (1952).

C. The Core Gyromagnetic Ratio

A value for the gyromagnetic ratio of the core g_R equal to Z/A follows if irrotational flow is assumed to dominate in the nucleus. Empirical evidence presently available for $2s$-$1d$ shell nuclei suggests $g_R \cong +0.3$ to be perhaps more realistic.[11] Although g_R may be expressed in relations involving the static nuclear magnetic-dipole moment, it has previously been noted that the uncertainty in mesonic contributions to the observed magnetic-dipole moment is sufficient to limit the accuracy of these relations.[3]

Since $J=\Omega=K=\frac{3}{2}$ for the ground states of Ne^{21} and Na^{23}, the relation

$$\mu=\frac{J}{J+1}\left\{(g_s-g_l)\left(\frac{a_{21}^2-a_{22}^2}{2}\right)+g_lJ+g_R\right\}, \quad (4)$$

wherein $a_{Nl}(\eta)$ are the normalized Nilsson eigenfunction coefficients associated with orbit 7, may be employed to evaluate μ as a function of g_R. As illustrated in Table II and in Fig. 6, the model predictions are fairly insensitive to the choice of g_R. In view of the uncertainty associated with the g_R parameter evaluation, subsequent computations were carried out both for $g_R=Z/A=+0.48$ and $g_R=+0.23$, the two values appearing to be reasonably generous extremes.

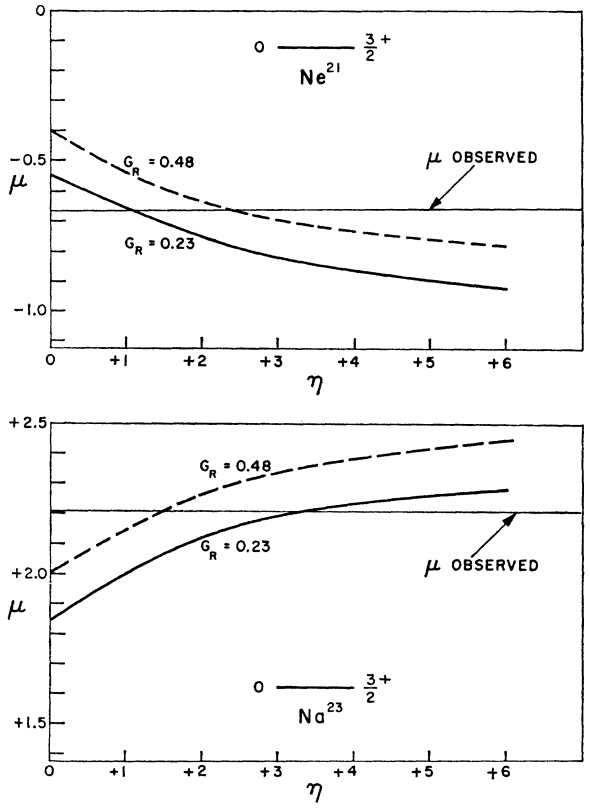

FIG. 6. The magnetic-dipole moments for the ground states of Ne^{21} (upper portion) and Na^{23} (lower portion) versus the core-deformation parameter η. The solid and dashed curves correspond to the Nilsson-model predictions with $g_R=0.23$ and 0.48, respectively. The cross-hatched regions indicate experimental observations reported in Refs. 33 and 34; the experimental uncertainties are less than the width of the lines. See also Table II.

D. Electromagnetic Transition Probability Expressions

It should perhaps be emphasized again that the considerations presented above are based upon the assumption that the *ground* states of Ne^{21}, Na^{21}, and Na^{23} may be interpreted as essentially pure K, π, $J=\frac{3}{2}$, $+$, $\frac{3}{2}$ configurations associated with Nilsson orbit 7 ($\Omega=\frac{3}{2}$), consistent with all previously reported collective-model studies.[1-9] Although similar purities for the description of the $\frac{5}{2}^+$ and $\frac{7}{2}^+$ excited states under discussion herein neither would be expected nor are in fact indicated by these previous studies, the states in question nonetheless appear to be successfully represented as predominantly $K^\pi=\frac{3}{2}^+$ rotational band members.

Since collective effects are anticipated to be most pronounced for intraband transitions,[35] neglect of possible band mixing in the $\frac{5}{2}^+$ and $\frac{7}{2}^+$ states as well as in the ground state should be a valid approximation in testing the validity of the model. In the analyses which follow, only the $K^\pi=\frac{3}{2}^+$ contribution for the first three states is considered, all transitions being treated as of intraband variety between states based upon Nilsson orbit 7.

The Nilsson expression[10] appropriate to the description of magnetic-dipole transitions between states with respective spins I and I' in the same rotational band associated with this orbit is

$$T(M1)=\frac{1}{3\hbar}\left(\frac{E\gamma}{\hbar c}\right)^3\left(\frac{e\hbar}{2Mc}\right)^2 \times|\langle I1\,\tfrac{3}{2}\,0|I1\,I'\,\tfrac{3}{2}\rangle|^2 G_{M1}^2\ \text{sec}^{-1}, \quad (5)$$

wherein $G_{M1}=3g_l-3g_R+(g_s-g_l)(a_{21}^2-a_{22}^2)$.

For the corresponding reduced electric-quadrupole transition probability the single-particle and collective contributions are included in the expression of McManus and Sharp[36]:

$$T(E2)=\frac{e^2}{15\hbar}\left(\frac{E\gamma}{\hbar c}\right)^5\left(\frac{\hbar}{M\omega_0}\right)^2 \times|\langle I2\,\tfrac{3}{2}\,0|I2\,I'\,\tfrac{3}{2}\rangle(1+y_{E2}{}^c)|^2 G_{E2}^2\ \text{sec}^{-1}, \quad (6)$$

where $G_{E2}=+0.5a_{21}^2-a_{22}^2$, $y_{E2}{}^c\simeq ZA^{1/3}\epsilon(1+\frac{1}{2}\epsilon)/G_{E2}$, and $\hbar\omega_0=41A^{-1/3}[1-\frac{1}{3}\epsilon^2-(2/27)\epsilon^3]^{-1/3}$ MeV.

[33] J. T. LaTourette, W. E. Quinn, and N. F. Ramsey, Phys. Rev. 107, 1202 (1957).

[34] *Nuclear Data Sheets*, compiled by K. Way (National Academy of Science–National Research Council, Washington 25, D. C.).

[35] D. A. Bromley, H. E. Gove, and A. E. Litherland, Can. J. Phys. 35, 1057 (1957).

[36] H. McManus and W. T. Sharp, as quoted in Ref. 35.

Neglecting octupole and higher order multipole contributions, the transitions under discussion herein are either $M1$-$E2$ mixtures or pure $E2$ in character; the probability for transitions from state i to state j is expressed as the sum of the relevant partial probabilities:

$$T_{ij} \equiv T_{ij}(M1) + T_{ij}(E2). \quad (7)$$

The square of the multipole-amplitude ratio associated with this de-excitation radiation is then generally defined as

$$\delta_{ij}^2 \equiv T_{ij}(E2)/T_{ij}(M1). \quad (8)$$

In situations where branching occurs from state i to two lower lying states j and j', respectively, the total transition probability associated with the gamma radiations from state i is given by the relation

$$T_i \equiv T_{ij} + T_{ij'}, \quad (9)$$

and the pertinent branching ratio is expressed as

$$\text{B.R.} = T_{ij'}/T_{ij}. \quad (10)$$

In the presentation to follow, the states i, j, and/or j' involved are labeled as the kth member of the rotational band ($k=1, 2, 3 \ldots$) as identified in Table I.

E. Relative Phases of Mixed Gamma Radiations

In contrast with the aforementioned nuclear parameters, the relative phase of coherently interfering radiations under the assumption of time-reversal invariance in a particular nuclear transition is discrete rather than continuously variable. Since it interrelates the reduced matrix elements representing the model states, the comparison of model-predicted and experimentally determined relative phases for a particular mixed transition is of fundamental importance in determining the validity of the model representation. Employing the phase convention suggested by Lloyd,[37] the amplitude mixing ratio for radiations L and L', which are assumed to interfere coherently in a given transition, is expressed in terms of the reduced matrix element as

$$\delta = \langle J_f \| L' \| J_i \rangle / \langle J_f \| L \| J_i \rangle, \quad (11)$$

where J_i and J_f represent the total angular momentum associated with the initial and final states, respectively, in the particular transition for which the amplitude mixing ratio is being determined.

The Nilsson model is presented employing this same convention.[10] Where appropriate, values of the multipole amplitude ratio previously presented using a different phase convention have been converted to the form of Eq. (11) via the relationship[38]

$$\frac{\langle J_f \| L' \| J_i \rangle}{\langle J_f \| L \| J_i \rangle} = (-1)^{L'-L} \frac{\langle J_i \| L' \| J_f \rangle}{\langle J_i \| L \| J_f \rangle}. \quad (12)$$

[37] S. P. Lloyd, Phys. Rev. 83, 716 (1951).

[38] L. C. Biedenharn, in *Nuclear Spectroscopy*, edited by F. Ajzenberg-Selove (Academic Press Inc., New York, 1960), Part B, Chap. V.C.

F. Relative Gamma-Ray Transition Probabilities and Phases

Employing Eqs. (5) and (6) above and utilizing values of κ and g_R consistent with the discussion given in Secs. IIIB and IIIC, the relative *partial* gamma-ray transition probabilities for six transitions of $M1$-$E2$ character interpreted herein as being of intraband variety have been examined in some detail. In accordance with Eq. (8), Figs. 7 and 8 display the model values

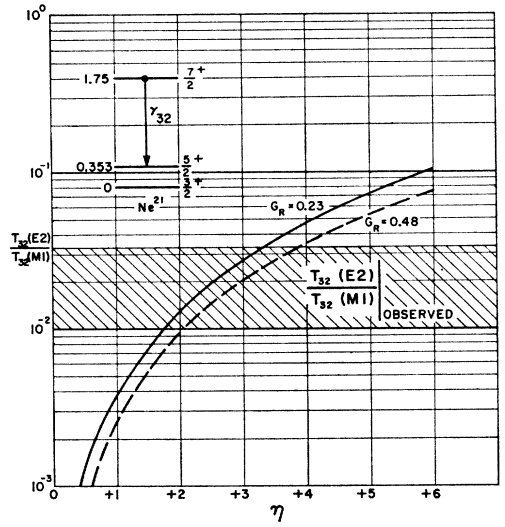

FIG. 7. Relative partial gamma-ray transition probabilities for the $\frac{7}{2}^+(1.75) \rightarrow \frac{5}{2}^+(0.353\text{-MeV})$ transition in Ne^{21} versus the core-deformation parameter η. The solid and dashed curves correspond to the Nilsson-model predictions with $g_R=0.23$ and 0.48, respectively, and with $\kappa=0.10$; the cross-hatched region indicates experimental observations reported in Ref. 14. See Table III for relative phase determinations.

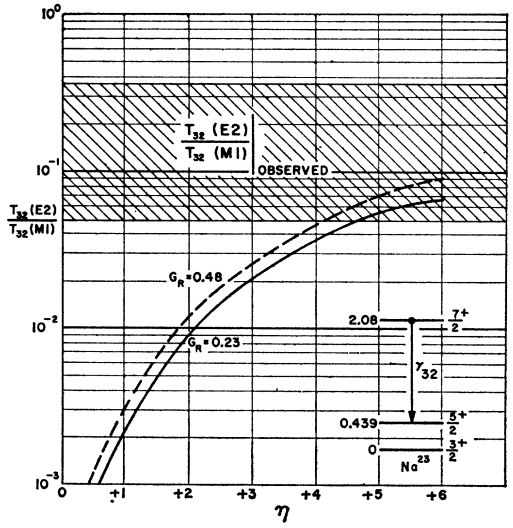

FIG. 8. Relative partial gamma-ray transition probabilities for $\frac{7}{2}^+(2.08) \rightarrow \frac{5}{2}^+(0.439\text{-MeV})$ transition in Na^{23} versus the core-deformation parameter η. Notation as in Fig. 7; experimental observation is the smaller of the two values reported in Refs. 22 and 29. See also Table III for relative phase determinations and the larger experimentally allowed value.

TABLE III. Relative partial gamma-ray transition probabilities and phases.

Nucleus	$T_{21}(E2)/T_{21}(M1)$ Relative phase[a] Observed	Ref.	Predicted[b] $g_R=0.23$	$g_R=0.48$	$T_{32}(E2)/T_{32}(M1)$ Relative phase[a] Observed	Ref.	Predicted[b] $g_R=0.23$	$g_R=0.48$
Ne^{21}	0.00046±0.00044	16	0.0066	0.0047	0.021±0.009		0.048	0.035
					180°	14		
	0°		180°	180°	0.012±0.008		180°	180°
					0°	15		
Na^{21}	0.0050±0.0050	23	0.0029	0.0038	···		0.023	0.030
	0°		0°	0°			0°	0°
Na^{23}	0.0022±0.0013	28	0.0056	0.0072	0.020±0.015		0.036	0.047
					or			
					4.0±2.2			
	0°		0°	0°	0°	29	0°	0°

[a] Phase convention defined in text, Sec. IIIE.
[b] Computed with $\eta=+4.0$ and $\kappa=0.10$.

for the square of the multipole amplitude ratio associated with the stop-over cascade radiations originating from the $k=2$, $\frac{7}{2}^+$ Ne^{21} and Na^{23} band members as functions of the deformation parameter η for $0\leq\eta\leq+6$. Also shown in these figures are the experimental values discussed in Sec. II. It is noted that these data are consistent, within reasonable accuracy, with a common nuclear deformation characterized by $\eta\simeq+4$. Selecting this value of the deformation parameter, a comparison between predicted and observed values for the relative partial transition probabilities under discussion is presented in Table III; agreement within a factor of 2 is noted in four of the five cases presently amenable to intercomparison for either chosen value of g_R discussed in Sec. IIIC. The exception involves the first-excited to the ground-state transition in Ne^{21}, where the observed value is approximately an order of magnitude smaller than the predicted value (*s*).

Equation (11) having been adopted in its definition, the predicted and observed relative phases of the assumed coherently interfering multipoles in each of the above transitions are also presented in Table III. Unambiguous agreement is obtained in three of the five cases amenable to intercomparison, while clear disagreement is noted in the case of the first-excited to ground-state transition in Ne^{21}. In the remaining case (the second- to first-excited-state transition in Ne^{21}), the relative phases determined by Howard *et al.*[14] and Pelte *et al.*,[15] which determinations are discussed in Sec. IIA, are in agreement and disagreement, respectively, with the model prediction. Despite experimental re-examination, no satisfactory explanation yet exists for the discrepancy between the experimental data in this case.

Applying considerations similar to those presented above, but in conjunction with Eq. (10) instead of

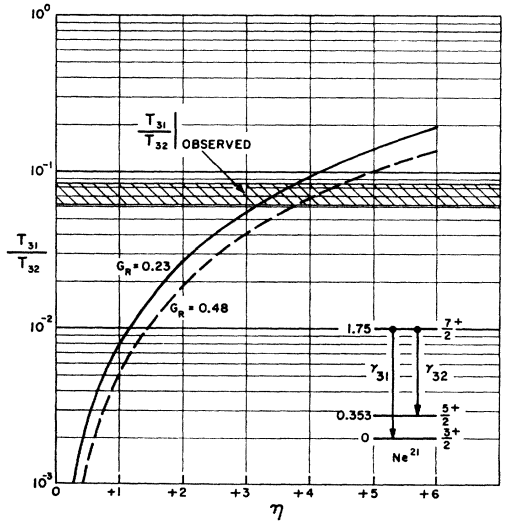

FIG. 9. Relative total gamma-ray transition probabilities for the $\frac{7}{2}^+$(1.75-MeV) state in Ne^{21} versus the core-deformation parameter η; $T_{31}=T_{31}(E2)$, $T_{32}=T_{32}(M1)+T_{32}(E2)$. Notation as in Fig. 7; experimental observations are those reported in Refs. 14 and 22. See also Table IV.

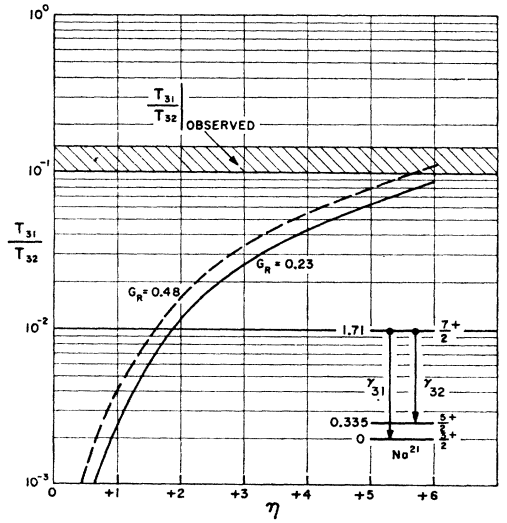

FIG. 10. Relative total gamma-ray transition probabilities for the $\frac{7}{2}^+$(1.71-MeV) state in Na^{21} versus the core-deformation parameter η. Notation as in Fig. 7; experimental observation is that reported in Refs. 21 and 22.

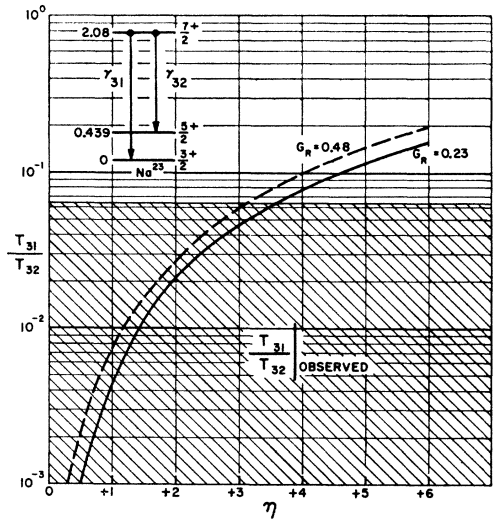

FIG. 11. Relative total gamma-ray transition probabilities for the $\frac{7}{2}^+$(2.08-MeV) state in Na^{23} versus the core-deformation parameter η. Notation as in Fig. 7; experimental observation is that reported in Refs. 22 and 29.

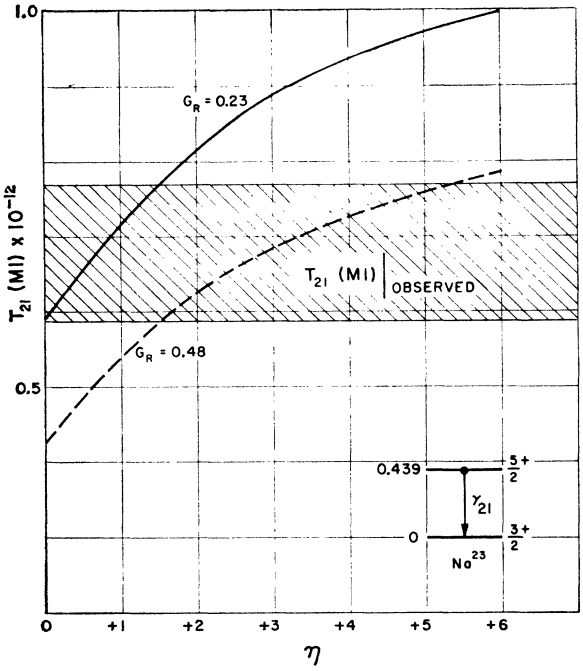

FIG. 12. Absolute magnetic-dipole gamma-ray transition probabilities for the $\frac{5}{2}^+$(0.439) $\rightarrow \frac{3}{2}^+$(0-MeV) transition in Na^{23} versus the core-deformation parameter η. The solid and dashed curves correspond to the Nilsson-model predictions with g_R=0.23 and 0.48, respectively; the cross-hatched region indicates experimental observations reported in Ref. 25. See also Table V.

Eq. (8), the relative *total* gamma-ray transition probabilities associated with the de-excitation of the $k=2$, $\frac{7}{2}^+$ states in Ne^{21}, Na^{21}, and Na^{23} have been computed for comparison with the observed branching ratios; Figs. 9, 10, and 11 display the results of the respective intercomparison for these three cases. Again it is apparent that a value $\eta\simeq+4$ provides the best single accord between model and experiment. Table IV presents a numerical comparison between predicted and observed branching ratios for $\eta=+4.0$; for either chosen value of g_R the agreement is within a factor of 2 in all three cases. Also presented in Table IV are the pertinent relative total transition probabilities associated with the de-excitation of the $k=3$, $\frac{9}{2}^+$ states postulated in Sec. II and summarized in Table I and Fig. 2; agreement similar to that noted above is observed for one of the two cases amenable to intercomparison.

In summary, the predicted values of the relative gamma-ray transition probabilities for assumed $K^\pi=\frac{3}{2}^+$ intraband transitions in $\zeta=11$ nuclear systems with $\eta=+4.0$, $\kappa=+0.10$, and $g_R=+0.23$ or $+0.48$ agree within a factor of 2 with seven of the eight well-established transitions in Ne^{21}, Na^{21}, and Na^{23} presently available for intercomparison. A preference between the two extreme values of g_R employed in the calculations cannot, however, be established from the experimental data. Clear disagreement concerning the relative phases of $M1$-$E2$ multipoles is noted in one of the five cases available for comparison. It is noteworthy that the *same* transition is involved in the disagreements regarding the relative partial gamma-ray transition probability and the relative phase, namely the first-excited to ground-state transition in Ne^{21}.

G. Absolute Gamma-Ray Transition Probabilities

Of the empirical observations on the absolute gamma-ray transition probabilities summarized in Sec. II, only three measurements are of sufficient precision for detailed intercomparison with the relevant model predictions: These intercomparisons are displayed in Figs. 12 and 13. As demonstrated in Table V, both the

TABLE IV. Relative total gamma-ray transition probabilities.

	T_{31}/T_{32}				T_{42}/T_{43}			
			Predicted[a]				Predicted[a]	
Nucleus	Observed	Ref.	g_R=0.23	g_R=0.48	Observed	Ref.	g_R=0.23	g_R=0.48
Ne^{21}	0.073±0.011	14	0.094	0.068	$\lesssim$1.0	14, 15	1.5	1.1
Na^{21}	0.122±0.022	22	0.044	0.055	···		0.71	0.88
Na^{23}	0.030±0.030	29	0.077	0.097	0.31±0.08	3	2.8	3.6

[a] Computed with η = +4.0 and κ =0.10.

TABLE V. Absolute partial gamma-ray transition probabilities.

Nucleus	$T_{21}(M1)$ (sec^{-1}) Observed	Ref.	Predicted[a] $g_R=0.23$	Predicted[a] $g_R=0.48$	$T_{21}(E2)$ (sec^{-1}) Observed	Ref.	Predicted[a] $\kappa=0.05$	Predicted[a] $\kappa=0.10$
Ne^{21}	$>1.6\times10^{10}$	18	2.0×10^{11}	2.8×10^{11}	1.1×10^{9}	19	0.28×10^{9}	1.3×10^{9}
Na^{21}	...		4.2×10^{11}	3.2×10^{11}	...		0.26×10^{9}	1.2×10^{9}
Na^{23}	5.5×10^{11}	25	9.4×10^{11}	7.3×10^{11}	2.3×10^{9}	26	1.1×10^{9}	5.3×10^{9}

[a] Computed with $\eta=+4.0$.

measured absolute magnetic-dipole and electric-quadrupole transition probabilities for the first-excited to ground-state de-excitations in Ne^{21} and Na^{23} are in good agreement, again within a factor of 2, with the model predictions for $\eta=+4.0$. Clearly, further observations of a more precise character than those presently reported on the (partial) lifetimes of the states in Ne^{21}, Na^{21}, and Na^{23} identified as higher lying band members (cf. Table I) are necessary in order to permit a more detailed intercomparison concerning absolute transition probabilities.

H. Beta-Ray Transition Probabilities

The treatment of Gamow-Teller–allowed beta transitions within the Nilsson model is analogous to that of magnetic-dipole gamma-ray transitions: The f_0t value for $\Delta J=0$, ±1 and $\Delta\pi=+1$ beta-transitions is expressed as

$$f_0t=B_0[(1-x)D_F(0)+xD_{GT}(0)]^{-1}, \qquad (13)$$

wherein $B_0=2787\pm70$ and $x=0.56\pm0.012$ are universal constants expressed in terms of their respective presently accepted values[39] and $D_F(0)$ and $D_{GT}(0)$ are the respective Fermi and Gamow-Teller–allowed transition matrix elements. For beta transitions between mirror nuclear states, $D_F(0)=1$; for Fermi-forbidden, Gamow-Teller–allowed $\Delta J=\pm1$ transitions, $D_F(0)=0$.

Since $D_{GT}(0)$ is expressed within the Nilsson-model formalism in terms of the a_{Nl} eigenfunctions employed for the magnetic-dipole transition probabilities, a comparison of observed[40,41] and predicted values of the associated $\log f_0t$ provides a further model test with regard to the pertinent eigenfunctions. It is further emphasized that these model predictions of f_0t values are independent of both the κ and g_R parameters discussed previously, and hence intercomparisons with the relevant observations should indicate the nuclear deformation more definitively than do the previously described gamma-ray transition probabilities considerations, which are functions of κ and/or g_R as well as η.

Once again, the model-predicted high purity of the states involved in the beta-transitions summarized in Table VI provides an excellent test for the validity of this simple model. The $\log f_0t$ values for "intraband" beta transitions, namely those involving initial and final states based upon Nilsson orbit 7, are depicted in Fig. 14, whereas the corresponding quantities for "interband" beta-transitions involving states based on Nilsson orbits 5 and 7 are presented in Fig. 15. The interpretation of the Ne^{23} ground state as being the lowest lying member of the $K^\pi=\frac{5}{2}^+$ rotational band is made from considerations on the static properties of $\zeta=13$ systems previously presented in detail.[12] Within the Nilsson model, computations of beta-ray transition probabilities can be carried out only between states having the same value for the nuclear deformation parameter.[10] For treating the Ne^{23} beta-decay, it is fortuitous that a nuclear deformation characterized by $\eta\simeq+4$ for the Ne^{23} ground state is indicated by these

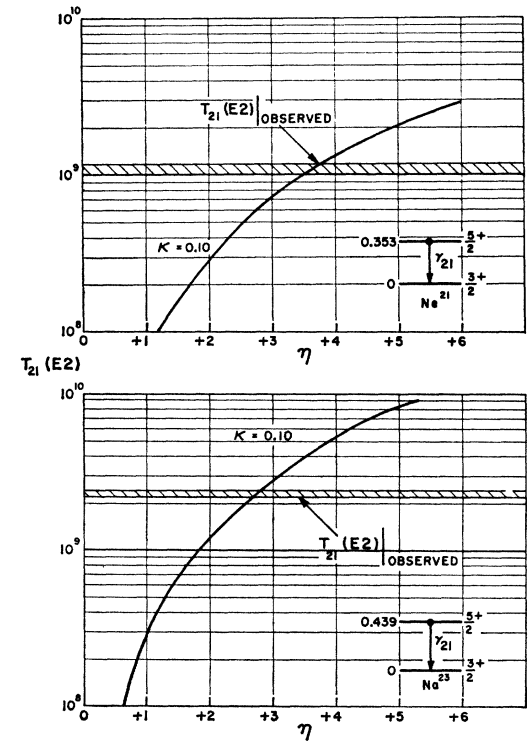

FIG. 13. Absolute electric-quadrupole gamma-ray transition probabilities for the $\frac{5}{2}^+(0.353)\rightarrow\frac{3}{2}^+(0\text{-MeV})$ Ne^{21} (upper portion) and $\frac{5}{2}^+(0.439)\rightarrow\frac{3}{2}^+(0\text{-MeV})$ Na^{23} (lower portion) transitions versus the core-deformation parameter η. The solid curves indicate the pertinent Nilsson-model predictions for $\kappa=0.10$; the cross-hatched regions indicate experimental observations reported in Refs. 19 and 26. See also Table V.

[39] M. E. Rose, in Ref. 38, Chap. V.D.
[40] W. L. Talbert and M. G. Stewart, Phys. Rev. **119**, 272 (1960).
[41] J. R. Penning and F. H. Schmidt, Phys. Rev. **105**, 647 (1957).

TABLE VI. Beta-ray transition probabilities.

Initial-state nucleus	J	K	Final-state nucleus	J'	K'	E_x' (MeV)	Logft Observed	Logft Ref.	Logft Predicted[a]
Na^{21}	$\frac{3}{2}^+$	$\frac{3}{2}$	Ne^{21}	$\frac{3}{2}^+$	$\frac{3}{2}$	0	3.59±0.06	40	3.60
Na^{21}	$\frac{3}{2}^+$	$\frac{3}{2}$	Ne^{21}	$\frac{5}{2}^+$	$\frac{3}{2}$	0.353	4.95±0.06	40	4.21
Ne^{23}	$\frac{5}{2}^+$	$\frac{5}{2}$	Na^{23}	$\frac{3}{2}^+$	$\frac{3}{2}$	0	5.3±0.1	41	5.11
Ne^{23}	$\frac{5}{2}^+$	$\frac{5}{2}$	Na^{23}	$\frac{5}{2}^+$	$\frac{5}{2}$	0.439	5.4±0.1	41	5.47[b]
Ne^{23}	$\frac{5}{2}^+$	$\frac{5}{2}$	Na^{23}	$\frac{7}{2}^+$	$\frac{5}{2}$	2.08	6.3±0.1	41	6.26
Mg^{23}	$\frac{3}{2}^+$	$\frac{3}{2}$	Na^{23}	$\frac{3}{2}^+$	$\frac{3}{2}$	0	3.74±0.01	40	3.60
Mg^{23}	$\frac{3}{2}^+$	$\frac{3}{2}$	Na^{23}	$\frac{5}{2}^+$	$\frac{3}{2}$	0.439	4.45±0.03	40	4.21

[a] Computed with $\eta = +4.0$.
[b] Computed with $D_F(0) \equiv 0$.

previous $\zeta = 13$ studies. With the exception of the mirror transition, the predicted values of logf_0t are seen in Figs. 14 and 15 to be sensitively dependent upon the deformation. The generally excellent agreement between observed and predicted values for logf_0t associated with the particular beta transitions summarized in Table VI, wherein the same value for the nuclear deformation parameter η has been employed (namely $\eta = +4.0$), provides additional support for the validity of both the general model representation and the value of the deformation parameter $\eta = +4.0$ for the three $\zeta = 11$ nuclei considered herein.

IV. CONCLUSION

Considerations of the observed static properties associated with the three lowest lying states in each of Ne^{21}, Na^{21}, and Na^{23} are all consistent with a collective-

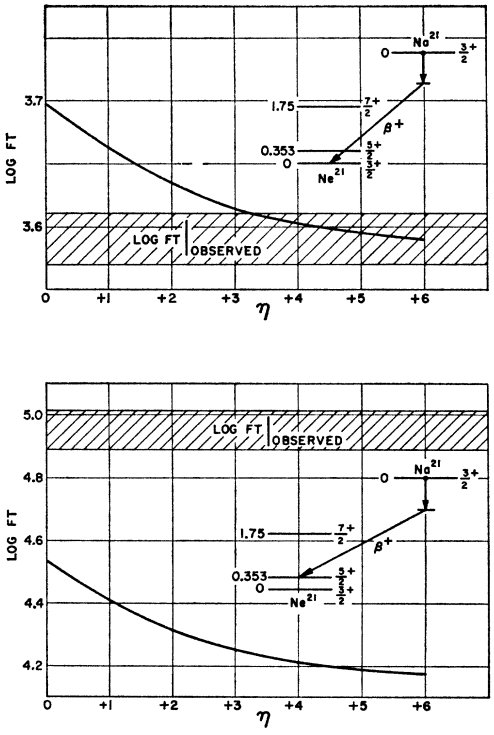

FIG. 14. Logft values for the β^+-decay of Na^{21} versus the core-deformation parameter η. Upper portion illustrates the Fermi and Gamow-Teller-allowed β^+ transition between the mirror ground states of Na^{21} and Ne^{21}; lower portion illustrates the Fermi-forbidden, Gamow-Teller-allowed β^+ transition from the $\frac{3}{2}^+$ Na^{21} ground state to the $\frac{5}{2}^+$(0.353-MeV)Ne^{21} state. The solid curves represent the Nilsson-model prediction, assuming identical values for the core-deformation parameter for the initial and final states in the β^+ transitions; the cross-hatched regions indicate experimental observations reported in Ref. 40. See also Table VI.

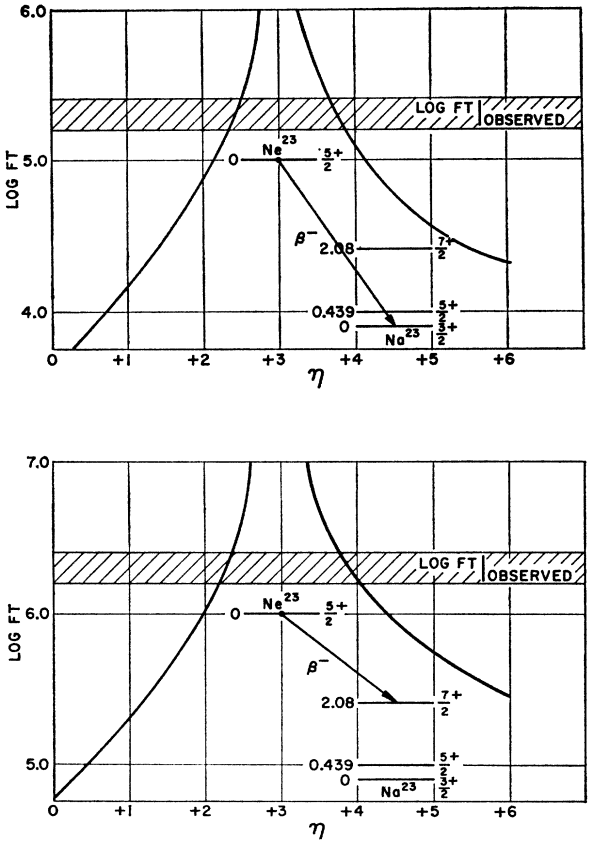

FIG. 15. Logft values for the β^- decay of Na^{23} versus the core-deformation parameter η. The β^- transitions from the $\frac{5}{2}^+$ Ne^{23} ground state to the $\frac{3}{2}^+$ Na^{23} ground state (upper portion) and $\frac{7}{2}^+$(2.08-MeV)Na^{23} state (lower portion) are interpreted as involving an initial state based on orbit 9 ($K^\pi = \frac{5}{2}^+$) and respective final states based on orbit 7: Identical values for the core-deformation parameter for the initial and final states in the β^- transitions are assumed. The cross-hatched regions indicate experimental observations reported in Ref. 41. See also Table VI.

model interpretation wherein a prolate deformation in the vicinity of $\eta=+4.0$ is indicated for each of these three $\zeta=11$ systems. Values for the spin-orbit coupling and core-gyromagnetic-ratio parameters pertinent to the description of the low-lying states in these three "central" $\zeta=11$ nuclear systems have been deduced from both ground-state static property and systematic behavior considerations: $\kappa=0.10$ and $0.23\leq g_R\leq 0.48$ are these respective values. Employing these parametric values and neglecting Coriolis coupling, we have shown that the predicted dynamic properties of the lowest lying states identified as predominantly $K^\pi=\frac{3}{2}^+$ rotational band members are all in reasonably good accord with the empirical data for a common nuclear deformation of $\eta\simeq+4$.

As illustrated in Figs. 7 through 15, the present experimental uncertainties (which are *not* uncommonly large) associated with the observed transition probabilities are of sufficient magnitude as to preclude the possibility of establishing differences between similar transitions in the three systems which might be ascribable to the difference in the effective charge of the assumed extra-core nucleon in Ne^{21} and $Na^{21}-Na^{23}$ and/or the difference in Coriolis coupling for $Ne^{21}-Na^{21}$ and Na^{23}. With regard to the first difference, it is noted that in the present interpretation, the stable nuclear deformation assumed, namely $\eta=+4.0$, corresponds to $y_{E2}{}^c\cong+40$ in Eq. (6). Therefore the collective, core contribution in essence completely accounts for the $E2$ enhancement, the charge of the extra-core nucleon being inconsequential in this interpretation of the electric-quadrupole transition probability. Concerning the second difference, in the light of the aforementioned experimental uncertainties the generally good agreement between observed dynamic properties and those predicted with complete omission of "contaminant" amplitudes in the pertinent wave functions appears to justify for the present said omission. Consequently, distinguishability of the $Ne^{21}-Na^{21}$ and the Na^{23} systems because of *differences* in Coriolis coupling therein would not be expected in the present comparison of dynamic properties.

The agreement between the predicted and observed relative phases in at least three and perhaps four of the five mixed intraband transitions intercompared is encouraging. It may well be significant that the transition in which the most severe disagreement between observed and predicted transition probabilities also corresponds to that one for which relatively well-established disagreement in relative phase of the interfering radiations occurs, namely the first-excited to ground-state transition in Ne^{21}. In comparison with the presently reported pertinent observation, this particular transition appears anomalous from the viewpoint of the Nilsson collective model.

Although the absolute $M1$ transition speed has not been measured as yet, the results of this intercomparison suggests that it is the $M1$ (and *not* the $E2$) transition probability which is more inaccurately predicted for the $0.353\rightarrow 0$-MeV Ne^{21} case; an enhancement factor of approximately one order of magnitude is indicated for this $M1$ transition. It will be of considerable interest to establish an experimental verification of and source for this apparent anomaly.

The fact that the agreement between model and observation is exceptionally good in the situations treated herein, which have been anticipated to be favorable from the model viewpoint, lends strong credibility to the basic tenets of the model. Further selective studies on the $\zeta=11$ nuclear systems are needed in order to provide the data for a more exact interpretation of these systems; such studies should be of particular significance in elucidating nuclear structure at the beginning of the $2s$-$1d$ nuclear shell.